Published in final edited form as:
J Infect Dis. 2009 July 15; 200(2): 307–313. doi:10.1086/599838.

Time course global gene expression analysis of an *in vivo Candida* biofilm

Jeniel E. Nett[1,3], **Alexander J. Lepak**[1], **Karen Marchillo**[1], and **David R. Andes**[1,2,*]

[1]Dept of Medicine, University of Wisconsin

[2]Dept of Medical Microbiology and Immunology, University of Wisconsin

[3]Dept of Cellular and Molecular Biology, University of Wisconsin

Abstract

Candida device infections are common and invariably associated with biofilm growth. Exploratory microarray studies were undertaken to identify target genes associated with biofilm formation from an *in vivo* catheter model over time. We compared mRNA levels from *C. albicans* grown in an *in vivo* central venous catheter biofilm model at 12h (intermediate growth) and 24h (mature) to *in vitro* planktonic cells without a biofilm substrate using *C. albicans* oligo-arrays. 124 transcripts were similarly upregulated at the 12 and 24h timepoints. Ontology categories most highly represented included energy/metabolism (12%), carbohydrate (10%) and protein (13%) synthesis and modification, and transport (6%). Numerous genes were previously identified from *in vitro* biofilm studies. These genes included those associated with hyphal growth, amino acid metabolism, adherence, drug resistance, ergosterol biosynthesis, and β-glucan synthesis. In the current data set, adherence genes were unique to the earlier timepoint. Differences between the current *in vivo* biofilm expression data and that previously reported from *in vitro* models, including alterations in metabolism and carbohydrate processing, may be due to the continuous availability of nutrients from host serum and the incorporation of the host-pathogen interaction.

INTRODUCTION

Candida albicans is an important human pathogen causing a wide spectrum of diseases and is a leading cause of nosocomial bloodstream infection. Candidemia is frequently associated with implantantion of a medical device. When growing on the surface, such as a venous catheter or urinary catheter, *Candida* adapts to a biofilm lifestyle [1, 2]. Biofilm growth involves phenotypic changes distinct from planktonic growth [3-5]. Two such characteristics, drug-resistance and reduced susceptibility to the host immune system, contribute to the difficulty in treating *Candida* biofilm infections. Greater understanding of the gene expression patterns present in *Candida* biofilms is one method to begin to discern the pathways important for the biofilm phenotype and identify potential antifungal targets.

Many *in vitro* model systems have been developed to mimic the biofilm growth found on infected medical devices. These models have provided the foundation for investigation of biofilm composition, architecture, and mechanisms of drug-resistance [3, 5, 6]. More recently, transcription profiling experiments have identified potential biochemical pathways required for biofilm formation [7-9]. Although the substratum common to these clinical infection sites (i.e. catheter, denture material) can be used *in vitro*, the models lack other environmental conditions potentially important in human infections [10]. In device-

*600 Highland Ave, Room H4.572 Madison, WI 53792 Ph: 608-263-1545 Fax: 608-263-4464 dra@medicine.wisc.edu .

associated infections, the substratum has been preconditioned with host proteins soon after implantation [1, 10]. This preconditioning film impacts biofilm formation and extracellular matrix production. *In vitro* models are not necessarily exposed to all the host proteins needed for the appropriate preconditioning film. Also, in many *in vitro* models, nutrients are depleted and waste products accumulate. However, *in vivo* biofilm cells are exposed to a continuous nutrient supply and waste products are eliminated while in the vasculature or other host tissue site [11]. Imaging of *in vivo* biofilms has also demonstrated incorporation of host cells, which may potentially impact biofilm formation. This host-pathogen interaction is not represented in these *in vitro* models. Finally, flow dynamics of host vasculature are difficult to reproduce *in vitro*.

In the current experiments, we utilize an *in vivo* rat catheter biofilm infection model [11]. This central venous catheter rat model mimics conditions encountered in human infections, including exposure to host proteins and immune components, host vasculature, and biofilm substratum. Inclusion of these variables in the model system allows us to account for the host-pathogen interaction and examine its impact on the transcriptional profile of *Candida* during biofilm development. The importance of the host-pathogen interaction, by use of *in vivo* model systems, has been previously demonstrated in study of both the host and pathogen transcriptomes [12]. The current study demonstrates the relevance and importance of incorporating the host infection site and immune system for the biofilm process.

METHODS

In vivo Venous Catheter Biofilm Formation

A *C. albicans* central venous catheter biofilm model was used for *in vivo* experiments as previously described [11, 13, 14]. Following catheter placement for 24h, a *C. albicans* SC5314 inoculum of 10^6 cells/ml in 0.15M NaCl was instilled in the catheter. Catheters were removed for RNA isolation or imaging following a 12 or 24h incubation. To yield a sufficient amount of RNA for the microarray analysis, *Candida* cells from 2-5 catheters were pooled. Collected cells were flash frozen with liquid nitrogen in AE buffer (50 mM sodium acetate pH 5.2, 10 mM EDTA) prior to RNA processing as previously described. RNA was collected using the hot method as previously described [11]. The RNA integrity was assessed using Agilent Bioanalyzer 2100 with a RNA Nanochip before use in microarrays.

Planktonic Culture Conditions

C. albicans SC5314 was propagated overnight in YPD at 37°C on orbital shaker at 250RPM and used for inoculation of planktonic cultures. Planktonic cultures were obtained in parallel with in vivo cultures by incubated the cells in 20 ml of RPMI in a glass flask at 37°C on orbital shaker at 250RPM. Log phase planktonic cells were harvested by centrifugation and the cells were flash frozen with liquid nitrogen in AE buffer until RNA processing. RNA was collected and integrity investigated as described above.

Biofilm Scanning Electron Microscopy (SEM)

Catheters were harvested at each timepoint for imaging as previously described [11]. Samples were imaged in a JEOL JSM-6100 in the high-vacuum mode at 10kV. The images were assembled using Adobe Photoshop 7.0.

Microarray and RT-PCR

C. albicans oligo microarray slides were purchased from the Biotechnology Research Institute, National Research Council, Montreal (Version Oligo Trial 2). Three biologic replicates and dye swaps were performed for each condition and timepoint as previously

described [12, 15, 16]. The microarrays were scanned with an Agilent DNA microarray scanner (G2565BA). Lowess normalization and statistical analysis were performed using Genespring v.7 (Agilent Technologies, CA). Genes whose expression was either increased 1.5-fold (log2) or decreased 0.67-fold for *C. albicans* biofilm samples relative to planktonic samples were considered for further analysis. A two-sided Student's *t* test was used determine the statistical significance of the log ratios.

Quantitative real-time reverse transcription-PCR (RT-PCR) was used to confirm mRNA abundances of a subset of upregulated transcripts from the microarray studies. The TaqMan probe and primer sets were designed using Primer Express (Applied Biosystems, Foster City, CA) (Table 1). The QuantiTect probe RT-PCR kit (Qiagen, Valencia, CA) was used in an ABI PRISM 7700 v1.7 sequence detection system (Applied Biosystems) as previously described. Reactions were performed in triplicate. The quantitative data analysis was completed using the C_t ($2^{-C}{}_t$) method [17]. The comparative expression method generated data as transcript fold-change normalized to a constitutive reference gene transcript (*ACT1*) and relative to a control or baseline condition.

RESULTS

In vivo Candida Biofilm Model

Images of the intermediate biofilm (12h) demonstrated yeast and hyphal cells attached to the substratum. At 24h, the mature biofilm consisted of an extensive network of yeast and hyphae embedded in strands of heterogeneous matrix material (Figure 1). Host cells, including red and white blood cells, were also embedded in the *Candida* biofilm.

Transcript Profiles of Intermediate and Mature *In vivo Candida* Biofilms

The genome-wide changes in gene expression in intermediate and mature *Candida* biofilms are shown in Supplemental Tables 1 and 2. From the intermediate biofilm and planktonic comparison, we identified 545 transcripts of the 6,354 ORFs (8.6%) as differentially regulated at least 1.5 fold. Within this group, 457 transcripts were upregulated during biofilm formation (biofilm/planktonic ratio greater than 1.5) and 88 transcripts were downregulated (biofilm/planktonic ratio less than 0.67). In the comparison of mature (24h) biofilm cells and planktonic cells, 1034 transcripts (16.3%) were differentially regulated. 523 transcripts were upregulated during mature biofilm formation and 511 transcripts were downregulated.

Of the genes differentially expressed in intermediate biofilm formation, multiple functional categories were represented (Table 2). During intermediate biofilm development, transcripts involved in protein synthesis (17%), transport (5%), stress (4%), amino acid metabolism (4%), cell wall metabolism (3%), energy and general metabolism (9%), and carbohydrate processing (7%) were abundant. The functions of 44% of the genes with transcriptional upregulation in intermediate biofilm formation have not yet been identified. Transcripts reduced during intermediate biofilm formation were primarily involved with DNA processing and cell cycle (19%), although changes in transcription and protein synthesis (10%), transport (5%), cytoskeleton (5%), and carbohydrate processing (6%) were also evident.

In the mature biofilm, we noted similar changes in gene regulation (Table 2). Again, multiple functional categories were represented. Transcription of genes associated with protein processing (17%), energy and metabolism (8%), transport (5%), DNA/cell cycle (5%), and carbohydrate processing (5%) was upregulated in the mature biofilm cells. Similar to the intermediate biofilm, mature biofilm formation was associated with reduction of transcripts involved in DNA processing and cell cycle (7%), transcription and protein

synthesis (13%), and transport (7%). The functions of near 40% of the differentially regulated genes are not yet known.

Next, we identified transcript abundance during both the intermediate biofilm and mature biofilm cells as a marker for relevance throughout the majority of biofilm formation. Transcript abundance of 124 genes was found at both the 12h and 24h timepoints, when compared to cells growing in planktonic conditions (Table 3). Genes involved in carbohydrate synthesis and processing (10%), transcription and protein synthesis (13%), and energy and metabolism (12%) were among those highly expressed at both timepoints. Transcripts involved in cell wall metabolism (4%), iron metabolism (3%) and amino acid metabolism (5%) were also abundant. Transcription of only 27 genes was downregulated in both the intermediate and mature biofilms (Table 4). Genes involved in DNA processing (30%) were most represented among the reducted transcripts.

Validation of Microarray Data by Real-time RT-PCR

Thirteen genes of interest were chosen to include several functional categories, including those involved in adherence, drug resistance, ergosterol synthesis, transport, amino acid metabolism, cell wall synthesis, and iron metabolism. We found that the expression direction for each gene chosen was consistent with the array data (Table 5).

DISCUSSION

Nearly all device-associated infections are associated with organisms growing as biofilms [1, 2, 18]. Most of our knowledge about *Candida* biofilms is based on in vitro studies, but such systems cannot completely simulate the environment of the infection site and host immune system. The in vivo central venous catheter model was developed to incorporate these experimental variables and has been shown useful for the investigation of *Candida* biofilm development, diagnosis, drug treatment and resistance, and study of the role of specific individual gene products [11, 13, 19, 20]. The current investigation expands the examination of the molecular basis for biofilm formation by assessing the temporal global transcript profile during *C. albicans* biofilm development.

These experiments identified differential regulation of many genes previously shown important in biofilm formation *in vitro* [4, 21-23]. Also, a subset of differentially expressed transcripts in the current *in vivo* study has been previously identified in genomic investigation of the planktonic *Candida* response to the mammalian host and specific host cells [12, 24]. Among the similarities to prior biofilm study was the upregulation of genes involved in adherence (*ALS1* and *ALS4*), cell wall metabolism (*ECE1, SAP5*), carbohydrate and general metabolism (*CGT, ICL1, MLS1, PCK1, PDK1*), and hyphal formation (*HWP2*).

Noteworthy, *in vivo* biofilm formation involved differential regulation of the glyoxylate cycle, which allows organisms to use two carbon molecules as an energy source. Transcripts for two enzymes of the glyoxylate cycle, *MSL1* and *ICL1*, encoding malate synthase and isocitrate lyase, were 2.4 and 2.3-fold more abundant in the mature biofilm. Increased expression of these genes has been described upon inoculation and infection of animal models *in vivo* and by phagocytosis [24, 25]. Mature biofilms are heterogeneous with cells presumably exposed to gradients of nutrients. Biofilm cells closest to the catheter surface may experience a decreased supply of glucose. Increased expression of the glyoxylate cycle potentially allows the cells to utilize additional carbon sources.

The current analysis identified several expression differences between the 12 and 24h biofilm timepoints. These differences may be accounted for by the stepwise morphologic and architectural changes during biofilm development or perhaps due to a change in

metabolic state or a quorum sensing process. Initial biofilm formation requires the attachment of yeast cells to a substratum [26, 27]. As expected, expression of a greater number and intensity of adherence genes was observed at the earlier 12h timepoint. *ALS* (agglutinin-like sequence) genes are a family of adhesins recognized to play a role in adherence and early biofilm formation [21, 28, 29]. In the current studies, transcript abundance of *ALS1* (12-fold) and *ALS2* (4-fold) was present only at the earlier timepoint. The current study did not observe a transcript abundance of *ALS3*. This result supports the hypothesis that adhesins may have overlapping functions in biofilm formation *in vivo*. Another, possibility is that *ALS3* may have been upregulated at a timepoint other than those examined in the current microarray analysis.

Upon initial cell adherence to a solid surface and the instigation of biofilm formation, genes involved in amino acid biosynthesis have been shown to be differentially regulated *in vitro* [7, 30]. Pathways involved in sulfur metabolism and regulation of methionine and cysteine biosynthesis are among those upregulated as early as 30 min following adhesion. In the current study, increased expression of *MET3* (1.6-fold), *MET10* (1.7-fold), *CYS3* (3-fold), and *CYS4* (1.7-fold) was detected in the intermediate biofilm. The specific role of these pathways in early biofilm formation has not yet been elucidated. *MET3* is a primary activator of sulfur assimilation in planktonic cells and is generally repressed in the presence of extracellular cysteine and methionine. However, transcript abundance of *MET3* has been identified in biofilm systems containing methionine and cysteine concentrations above that normally needed for repression [30]. Although it is possible that amino acids are limited within microenvironments in a heterogeneous biofilm, the swift upregulation of these pathways upon adherence to a solid surface suggests a role in sensing and responding to the surface [30]. In contrast to the intermediate biofilm, changes in expression of genes involved in methionine and cysteine biosynthesis were not predominant in the mature phase of biofilm growth. Instead, abundance of transcripts encoding amino acid permeases (*DAO2*, *DIP5*, *GAP6*, and *GNP1*) was noted [31, 32].

Mature *Candida* biofilms are marked by a basal layer of yeast cells with subsequent layering of filamentous morphotypes and extensive matrix production [33]. Transition to the hyphal morphology intuitively requires differential regulation of hyphal-associated genes [20, 34]. The current studies identified expression of a number of hyphal-associated genes in both the intermediate (15 genes) and the mature biofilms (40 genes). Furthermore, transcription of *TEC1*, a transcription factor involved in hyphal morphogenesis, was upregulated (2.4-fold) in the mature biofilm [35]. Of note, we also identified downregulation (2.5-fold) of *TUP1*, a negative regulator of hyphal formation [9, 36].

Recent studies have identified quorum sensing molecules in *Candida* similar to those described in bacterial biofilm systems [37, 38]. Farnesol acts to inhibit formation of biofilm, while tyrosol induces replication and hyphal morphogenesis at low cell densities [39, 40]. *CHK1*, a histidine kinase gene, appears to be a component of the farnesol quorum sensing pathway because the *chk1/chk1* mutant is unresponsive to the action of farnesol [41]. In the current study, the *CHK1* transcript was abundant (1.8-fold) in the mature biofilm, but not the intermediate biofilm. This timing is consistent with *CHK1* involvement in the regulation of mature biofilms and perhaps not surprising given the much greater burden of organisms in the milieu at this later phase of development. A recent microarray analysis compared the transcriptome of a 24h mature biofilm exposed to farnesol to an unexposed biofilm and identified 274 differentially regulated transcripts [9]. Genes involved in hyphal morphology, drug resistance, and cell wall maintenance were highly represented. Sixty-nine of these farnesol-responsive genes were differentially regulated in the mature biofilm of the current study (Supplemental Table 3) [9].

We also identified altered regulation of ergosterol β-glucan pathways associated during in vivo biofilm growth. Similar changes in gene regulation have been recently described in the most basal layer of in vitro biofilm cells, blastospores [23]. When compared to the current studies, both identified increased transcripts of *ERG25* and β-1,6 glucan synthesis genes *KRE1* and *SKN1* (25). ERG25 is putative C-4 methyl sterol oxidase with a role in C4-demethylation of ergosterol biosynthesis intermediates. It has been proposed that this upregulation may allow for increased conversion of lanosterol to nonergosterol intermediates, including eburicol and 14-methyl fecosterol, at the expense of conversion to ergosterol [23, 42].

Additionally, altered expression of the β-1,3 glucan synthesis and modification pathways (*FKS1, BGL2, XOG1, PHR2, FEN1, GDB1,* and *SGA1*) was prominent in the current study [43, 44].. It has been hypothesized that the glucan pathway may restructure the biofilm cell wall and contribute to the drug resistant phenotype [23]. The β-glucan pathway may also play a role in biofilm matrix production. Formation of a mature biofilm requires production of an extracellular polymeric matrix, which is composed primarily of carbohydrate, glucose, and protein with smaller amounts of hexosamine and phosphorus [3, 18]. The presence of glucan molecules in secreted *Candida* biofilm material and their possible role in biofilm resistance has recently been reported [45]. A number of transcripts involved in carbohydrate processing and synthesis (44) and cell wall metabolism (40) were differentially expressed in the mature biofilm. These gene products may participate in production of matrix material. Interestingly, transcripts involved in the β-1,3 glucan degradation pathway (*ENG1* and *SWC1*) were reduced at the 24h timepoint. Both gene products, ENG1 and SWC1, have β-1,3 glucosidase activity. Disruption of *CaENG1* results in decreased β-1,3 glucanase activity 8]. It is possible that downregulation of these β-1,3 glucosidases and altered regulation of the β-1,3 glucan pathway may serve to conserve glucans for construction of a mature biofilm matrix.

Many factors have been proposed to contribute to *Candida* biofilm drug resistance, including upregulation of efflux pumps, decreased perfusion of antimicrobials through the matrix, slow growth, and alterations in plasma membrane ergosterol content [46, 47]. Early biofilm resistance coincides with increased transcript levels of efflux pumps *MDR1* and *CDR1* [48]. The current studies identified transcript upregulation of *CDR2* at 12h (1.5-fold) and *MDR1* at both 12h (2.1-fold) and 24h (1.9-fold). *PDR16* transcript abundance was also noted in both the intermediate (2.2-fold) and mature biofilms (3.7-fold). *PDR16* encodes a phosphatidylinositol transfer protein of the Sec14p family and is upregulated in fluconazole-resistant cells overexpressing *CDR1* and *CDR2* [49].

Candida biofilm resistance is likely multifactorial, with contributions from efflux pumps, ergosterol changes, matrix and other, not yet identified, processes. In more mature biofilms, changes in the ergosterol content of the plasma membrane have been hypothesized to contribute to biofilm resistance [4]. The ergosterol content of cells in a mature biofilm is 50% less than that found in an early-phase biofilm. The current studies observed altered regulation of the ergosterol pathway, as noted above.

Three prior studies have examined the global transcriptional response during *Candida* biofilm development [7, 9, 30]. The report with the most expression similarities to the current study was that which utilized a perfused model with continued nutrient repletion [7]. Forty-nine genes were differentially regulated in both the perfused model and current study (Supplemental Table 3). Similar to the perfused model, the current study found differential regulation of numerous amino acid synthesis genes in both the intermediate biofilms (18 genes) and mature biofilms (21 genes). The similarities of these models may, in part, be due to the unlimited supply of nutrients.

Similarities were also noted in comparison to an *in vitro* biofilm transcriptional profiling study utilizing a polystyrene petri dish as a substrate in a static condition with regard to nutrient supply [30]. This study focused on the early phase of *Candida* biofilm formation and might best be compared to the intermediate (12h) biofilm from the current study. Transcripts involved in sulfur metabolism (*MET3, MET10*) were abundant in both studies (Supplemental Table 3). Also, transcription of *NCE103*, a carbonic anhydrase-like gene, was upregulated in both biofilm models and may represent response to the metabolic state of the cells growing in a biofilm.

Analysis of the *in vivo* data set also identified differences from the *in vitro* transcriptional studies [7, 30]. For example, transcripts of genes encoding glucose transporters were among those most abundant at both timepoints. , Increased expression of both *HGT1* (5.4-fold) and *HGT2* (52-fold) was observed in intermediate biofilms. Mature biofilm formation was associated with transcriptional abundance of *HGT1* (4.7-fold), *HGT2* (7.6 fold), *HGT14* (2.2-fold), *HGT15* (5-fold), and *HGT19* (4.5-fold). One possible explanation for this expression is the need for scavenging glucose for nutrient-starved biofilm cells. Another possibility is a glucose requirement for production of the carbohydrate matrix.

A sizable subset of genes was differentially regulated in both the intermediate (8.5%) and mature (16%) biofilms. Genes involved in amino acid metabolism (*AGP2, ARG1, CAN1, CDG1, CPA1, CPA2*, and *SMM1*), cell wall metabolism (*BGL2* and *ECE1*), iron metabolism (*CFL2, FRE10, ISU1*, and *SIT1*), and drug resistance (*ERG25, PDR16* and *MDR1*) were among those abundant during the time periods examined (Table 3). We suspect these gene products may play a role in the biofilm phenotypes exhibited throughout the biofilm lifestyle, including drug resistance, cell wall changes, altered metabolism, and maintaining cell attachment.

Of note, the study did not identify differential expression of several genes of demonstrated importance in biofilm formation (*ADH1, BCR1, CPH1, EGF1, MKC1*, and *YWP1*) [19, 21, 34, 50]. The timing of expression of these genes may not correlate with the timepoints examined in our study. For example, *BCR1* and *ALS3* may play a role in earlier biofilm formation. Also, the magnitude of the differences in transcript level may be below that detectable by our microarray analysis or regulation may occur at the post-transcriptional level. The absence of these genes in the current data set points to the importance of time course experimentation.

The identification of transcripts unique to the current study demonstrates the value of *in vivo* models that more closely mimics the disease state. The data set provides a resource for laboratories to guide directed biofilm investigations and target specific gene products.

Supplementary Material

Refer to Web version on PubMed Central for supplementary material.

Acknowledgments

The project described was supported by Grant Number RO1 AI073289-01. The content is solely the responsibility of the authors and does not necessarily represent the official views of the National Institutes of Health.

REFERENCES

1. Kojic EM, Darouiche RO. *Candida* infections of medical devices. Clin Microbiol Rev. 2004; 17:255–67. [PubMed: 15084500]

2. Douglas LJ. *Candida* biofilms and their role in infection. Trends Microbiol. 2003; 11:30–6. [PubMed: 12526852]
3. Baillie GS, Douglas LJ. Matrix polymers of *Candida biofilms* and their possible role in biofilm resistance to antifungal agents. J Antimicrob Chemother. 2000; 46:397–403. [PubMed: 10980166]
4. Mukherjee PK, Chandra J, Kuhn DM, Ghannoum MA. Mechanism of fluconazole resistance in *Candida albicans* biofilms: phase-specific role of efflux pumps and membrane sterols. Infect Immun. 2003; 71:4333–40. [PubMed: 12874310]
5. Ramage G, Bachmann S, Patterson TF, Wickes BL, Lopez-Ribot JL. Investigation of multidrug efflux pumps in relation to fluconazole resistance in *Candida albicans* biofilms. J Antimicrob Chemother. 2002; 49:973–80. [PubMed: 12039889]
6. Chandra J, Kuhn DM, Mukherjee PK, Hoyer LL, McCormick T, Ghannoum MA. Biofilm formation by the fungal pathogen *Candida albicans*: development, architecture, and drug resistance. J Bacteriol. 2001; 183:5385–94. [PubMed: 11514524]
7. Garcia-Sanchez S, Aubert S, Iraqui I, Janbon G, Ghigo JM, d'Enfert C. *Candida albicans* biofilms: a developmental state associated with specific and stable gene expression patterns. Eukaryot Cell. 2004; 3:536–45. [PubMed: 15075282]
8. Esteban PF, Rios I, Garcia R, et al. Characterization of the *CaENG1* gene encoding an endo-1,3-beta-glucanase involved in cell separation in *Candida albicans*. Curr Microbiol. 2005; 51:385–92. [PubMed: 16328626]
9. Cao YY, Cao YB, Xu Z, et al. cDNA microarray analysis of differential gene expression in *Candida albicans* biofilm exposed to farnesol. Antimicrob Agents Chemother. 2005; 49:584–9. [PubMed: 15673737]
10. Nett J, Andes D. *Candida albicans* biofilm development, modeling a host-pathogen interaction. Curr Opin Microbiol. 2006; 9:340–5. [PubMed: 16815078]
11. Andes D, Nett J, Oschel P, Albrecht R, Marchillo K, Pitula A. Development and characterization of an in vivo central venous catheter *Candida albicans* biofilm model. Infect Immun. 2004; 72:6023–31. [PubMed: 15385506]
12. Andes D, Lepak A, Pitula A, Marchillo K, Clark J. A simple approach for estimating gene expression in *Candida albicans* directly from a systemic infection site. J Infect Dis. 2005; 192:893–900. [PubMed: 16088840]
13. Nett J, Lincoln L, Marchillo K, Andes D. Beta -1,3 glucan as a test for central venous catheter biofilm infection. J Infect Dis. 2007; 195:1705–12. [PubMed: 17471441]
14. Nett J, Lincoln L, Marchillo K, et al. Putative role of beta-1,3 glucans in *Candida albicans* biofilm resistance. Antimicrob Agents Chemother. 2007; 51:510–20. [PubMed: 17130296]
15. Lepak A, Nett J, Lincoln L, Marchillo K, Andes D. Time course of microbiologic outcome and gene expression in *Candida albicans* during and following in vitro and in vivo exposure to fluconazole. Antimicrob Agents Chemother. 2006; 50:1311–9. [PubMed: 16569846]
16. Nobile CJ, Solis N, Myers CL, et al. *Candida albicans* transcription factor Rim101 mediates pathogenic interactions through cell wall functions. Cell Microbiol. 2008
17. Livak KJ, Schmittgen TD. Analysis of relative gene expression data using real-time quantitative PCR and the 2(-Delta Delta C(T)) Method. Methods. 2001; 25:402–8. [PubMed: 11846609]
18. Donlan RM. Biofilm formation: a clinically relevant microbiological process. Clin Infect Dis. 2001; 33:1387–92. [PubMed: 11565080]
19. Mukherjee PK, Mohamed S, Chandra J, et al. Alcohol dehydrogenase restricts the ability of the pathogen *Candida albicans* to form a biofilm on catheter surfaces through an ethanol-based mechanism. Infect Immun. 2006; 74:3804–16. [PubMed: 16790752]
20. Nobile CJ, Nett JE, Andes DR, Mitchell AP. Function of *Candida albicans* adhesin Hwp1 in biofilm formation. Eukaryot Cell. 2006; 5:1604–10. [PubMed: 17030992]
21. Nobile CJ, Andes DR, Nett JE, et al. Critical role of Bcr1-dependent adhesins in *C. albicans* biofilm formation in vitro and in vivo. PLoS Pathog. 2006; 2:e63. [PubMed: 16839200]
22. Zhao X, Oh SH, Yeater KM, Hoyer LL. Analysis of the *Candida albicans* Als2p and Als4p adhesins suggests the potential for compensatory function within the Als family. Microbiology. 2005; 151:1619–30. [PubMed: 15870470]

23. Khot PD, Suci PA, Miller RL, Nelson RD, Tyler BJ. A small subpopulation of blastospores in *Candida albicans* biofilms exhibit resistance to amphotericin B associated with differential regulation of ergosterol and beta-1,6-glucan pathway genes. Antimicrob Agents Chemother. 2006; 50:3708–16. [PubMed: 16966398]
24. Fradin C, Kretschmar M, Nichterlein T, Gaillardin C, d'Enfert C, Hube B. Stage-specific gene expression of *Candida albicans* in human blood. Mol Microbiol. 2003; 47:1523–43. [PubMed: 12622810]
25. Lorenz MC, Fink GR. The glyoxylate cycle is required for fungal virulence. Nature. 2001; 412:83–6. [PubMed: 11452311]
26. Kumamoto CA, Vinces MD. Alternative *Candida albicans* lifestyles: growth on surfaces. Annu Rev Microbiol. 2005; 59:113–33. [PubMed: 16153165]
27. Hawser SP, Douglas LJ. Biofilm formation by *Candida* species on the surface of catheter materials in vitro. Infect Immun. 1994; 62:915–21. [PubMed: 8112864]
28. Richard ML, Nobile CJ, Bruno VM, Mitchell AP. *Candida albicans* biofilm-defective mutants. Eukaryot Cell. 2005; 4:1493–502. [PubMed: 16087754]
29. Nobile CJ, Schneider HA, Nett JE, et al. Complementary adhesin function in *C. albicans* biofilm formation. Curr Biol. 2008; 18:1017–24. [PubMed: 18635358]
30. Murillo LA, Newport G, Lan CY, Habelitz S, Dungan J, Agabian NM. Genome-wide transcription profiling of the early phase of biofilm formation by *Candida albicans*. Eukaryot Cell. 2005; 4:1562–73. [PubMed: 16151249]
31. Regenberg B, Holmberg S, Olsen LD, Kielland-Brandt MC. Dip5p mediates high-affinity and high-capacity transport of L-glutamate and L-aspartate in *Saccharomyces cerevisiae*. Curr Genet. 1998; 33:171–7. [PubMed: 9508791]
32. Regenberg B, During-Olsen L, Kielland-Brandt MC, Holmberg S. Substrate specificity and gene expression of the amino-acid permeases in *Saccharomyces cerevisiae*. Curr Genet. 1999; 36:317–28. [PubMed: 10654085]
33. Hawser SP, Baillie GS, Douglas LJ. Production of extracellular matrix by *Candida albicans* biofilms. J Med Microbiol. 1998; 47:253–6. [PubMed: 9511830]
34. Ramage G, VandeWalle K, Lopez-Ribot JL, Wickes BL. The filamentation pathway controlled by the Efg1 regulator protein is required for normal biofilm formation and development in *Candida albicans*. FEMS Microbiol Lett. 2002; 214:95–100. [PubMed: 12204378]
35. Schweizer A, Rupp S, Taylor BN, Rollinghoff M, Schroppel K. The TEA/ATTS transcription factor CaTec1p regulates hyphal development and virulence in *Candida albicans*. Mol Microbiol. 2000; 38:435–45. [PubMed: 11069668]
36. Braun BR, Johnson AD. Control of filament formation in *Candida albicans* by the transcriptional repressor TUP1. Science. 1997; 277:105–9. [PubMed: 9204892]
37. Hornby JM, Jensen EC, Lisec AD, et al. Quorum sensing in the dimorphic fungus *Candida albicans* is mediated by farnesol. Appl Environ Microbiol. 2001; 67:2982–92. [PubMed: 11425711]
38. Oh KB, Miyazawa H, Naito T, Matsuoka H. Purification and characterization of an autoregulatory substance capable of regulating the morphological transition in *Candida albicans*. Proc Natl Acad Sci U S A. 2001; 98:4664–8. [PubMed: 11274356]
39. Ramage G, Saville SP, Wickes BL, Lopez-Ribot JL. Inhibition of *Candida albicans* biofilm formation by farnesol, a quorum-sensing molecule. Appl Environ Microbiol. 2002; 68:5459–63. [PubMed: 12406738]
40. Chen H, Fujita M, Feng Q, Clardy J, Fink GR. Tyrosol is a quorum-sensing molecule in *Candida albicans*. Proc Natl Acad Sci U S A. 2004; 101:5048–52. [PubMed: 15051880]
41. Kruppa M, Krom BP, Chauhan N, Bambach AV, Cihlar RL, Calderone RA. The two-component signal transduction protein Chk1p regulates quorum sensing in *Candida albicans*. Eukaryot Cell. 2004; 3:1062–5. [PubMed: 15302838]
42. Barker KS, Crisp S, Wiederhold N, et al. Genome-wide expression profiling reveals genes associated with amphotericin B and fluconazole resistance in experimentally induced antifungal resistant isolates of *Candida albicans*. J Antimicrob Chemother. 2004; 54:376–85. [PubMed: 15201233]

43. Sarthy AV, McGonigal T, Coen M, Frost DJ, Meulbroek JA, Goldman RC. Phenotype in *Candida albicans* of a disruption of the *BGL2* gene encoding a 1,3-beta-glucosyltransferase. Microbiology. 1997; 143(Pt 2):367–76. [PubMed: 9043114]
44. Mio T, Adachi-Shimizu M, Tachibana Y, et al. Cloning of the *Candida albicans* homolog of *Saccharomyces cerevisiae GSC1/FKS1* and its involvement in beta-1,3-glucan synthesis. J Bacteriol. 1997; 179:4096–105. [PubMed: 9209021]
45. Nett J, Lincoln L, Marchillo K, et al. Putative Role of {beta}-1,3 glucans in *Candida albicans* Biofilm Resistance. Antimicrob Agents Chemother. 2007; 51:510–520. [PubMed: 17130296]
46. Ramage G, Saville SP, Thomas DP, Lopez-Ribot JL. *Candida* biofilms: an update. Eukaryot Cell. 2005; 4:633–8. [PubMed: 15821123]
47. Kuhn DM, Ghannoum MA. *Candida* biofilms: antifungal resistance and emerging therapeutic options. Curr Opin Investig Drugs. 2004; 5:186–97.
48. Mateus C, Crow SA Jr. Ahearn DG. Adherence of *Candida albicans* to silicone induces immediate enhanced tolerance to fluconazole. Antimicrob Agents Chemother. 2004; 48:3358–66. [PubMed: 15328097]
49. Saidane S, Weber S, De Deken X, St-Germain G, Raymond M. *PDR16*-mediated azole resistance in *Candida albicans*. Mol Microbiol. 2006; 60:1546–62. [PubMed: 16796687]
50. Kumamoto CA. A contact-activated kinase signals *Candida albicans* invasive growth and biofilm development. Proc Natl Acad Sci U S A. 2005; 102:5576–81. [PubMed: 15800048]

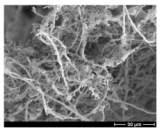

Figure 1.
Scanning electron micrograph of *C. albicans in vivo* biofilm. *C. albicans* SC5314 was inoculated into a rat venous catheter and allowed to dwell for 24h. Catheters were placed in a fixative, treated with osmium tetroxide and dehydrated through a series of ethanol washes and critical point drying.

Table 1

Primers used for RT-PCR experiments

Gene	Primers	Probe
ALS1	Forward: 5′ -TTAGCATCTGCAAGTGAAGAAGACA Reverse: 5′ -ATGGAGCTTCTGTAGGACTGGTTG	5 ′-/56-FAM/AGCGGTTCTCATGAATCAGCATCCACAA/36-TAMSp
ARG1	Forward: 5′ -GTGAAGTTAGAGCCATCAGAGATCAA Reverse: 5′ -TGAACGAACGTATTCTCCTTCTGG	5′ -/56-FAM/TTGTGACACCAACTTGGGCCAAAATCTT/36-TAMSp
BGL2	Forward: 5′ –CTCGCAACTGTTCTTACTTCAGTTG Reverse: 5′ -TGACGTCTTTACAAGTACCGTCATC	5′ -/56-FAM/TGAAAGCCAAATCACCCATGGCG/36-TAMSp
CDR2	Forward: 5′ -CCACATGTCCGACATACCTGG Reverse: 5′ -GGAATCTGGGTCTAATTGTTCATGA	5′ -/56-FAM/CCATTCAACGGCAACAT/36-TAMSp
ECM3	Forward: 5′ -TCCACAGTGAAGGGTCAGCTG Reverse: 5′ -CGCAAATCGCTTGTCCTAGAA	5′ -/56-FAM/AAGACGCCGTACATCAAATGCATCTGAACT/36-TAMSp
ERG25	Forward: 5′ -TGGATTGGCAGCAGAATATGC Reverse: 5′ -GCAAGTTACCAGTGATAAGACACCA	5′ -/56-FAM/CAATCGGAATACCAACCGTACCCAATCCTA/36-TAMSp
FET3	Forward: 5′ -TCGGTGTGTCATGGGAAGGTA Reverse: 5′ -ACCTCTAGCAGTGAAACCAGTTGG	5′ -/56-FAM/TGCCGCCGCCAACAGTAAAGACTACTT/36-TAMSp
HGT2	Forward: 5′ -AGGTCAATGGGAAGCTGCTG Reverse: 5′ -TAGCGTATCCAATATGCTTGCTTG	5′ -/56-FAM/CACGATCACCATGAGCTTGAACCTTGG/36-TAMSp
INO1	Forward: 5′ -GTCTTACTGGCTCAAGGCTCCA Reverse: 5′ -CCAACACTGAAAGCAAGTTGACTAA	5′ -/56-FAM/AGCAAGACCAGGATTCAAACCTATCAACGG/36TAMSp
KRE1	Forward: 5′ -GGCAGATAAAACATCCAGTTCAGTATC Reverse: 5′ -CCCAATCCAATAGAACCAGACG	5′ -/56-FAM/TTTCCCATTGGCATCAGTACCTGTGACC/36-TAMSp
PCK1	Forward: 5′ -TACTCTGGTAACAAAACCGGTAGATC Reverse: 5′ -ACTTGTTTATTCACTGGACCCCA	5′ -/56-FAM/TGTCGACGAATCCACCTCATCCCAT/36-TAMSp
PHR1	Forward: 5′ -CTGCAAAGCTGTTAGTGGAGTAGC Reverse: 5′ -TGATGATCCAGAAGTAGATGCAGAG	5′ -/56-FAM/TCCTCTGGTGGAAGCTCCAAATCTGG/36-TAMSp
SAP5	Forward: 5′ -CCAGATGATCCAACTGTTGAAGC Reverse: 5′ -TCCACATCACCATCTCTACCAGTC	5′ -/56-FAM/AGTTTACTCCCTCAGAATTTCCCGTCGATG /36-TAMSp
ACT1	Forward: 5′ -AGCTTTGTTCAGACCAGCTGATT Reverse: 5′ -GGAGTTGAAAGTGGTTTGGTCAA	5′ - /56-FAM/CCAGCAGCTTCCAAACCT/36-TAMSp

Table 2

Frequency distribution of differentially expressed genes among functional categories

Description	No. of genes in functional category (%)			
	Biofilm Upregulated 12 h	Biofilm Downregulated 12 h	Biofilm Upregulated 24 h	Biofilm Downregulated 24 h
Amino Acid	18 (4)	2 (2)	21 (4)	15 (3)
Carbohydrate	30 (7)	5 (6)	27 (5)	17 (3)
Cell Wall	15 (3)	3 (3)	22 (4)	18 (4)
Cytoskeleton	2 (0)	4 (5)	5 (1)	15 (3)
DNA/Cell Cycle	10 (2)	17 (19)	24 (5)	38 (7)
Energy/Metabolism	41 (9)	1 (1)	40 (8)	28 (5)
Fatty Acid	6 (1)	0 (0)	3 (1)	0 (0)
Heat Shock Protein	1 (0)	0 (0)	3 (1)	0 (0)
Hyphal	4 (1)	3 (3)	8 (2)	6 (1)
Iron	9 (2)	0 (0)	9 (2)	4 (1)
Plasma Membrane	2 (0)	3 (3)	15 (3)	13 (3)
Resistance/Stress	20 (4)	2 (2)	9 (2)	10 (2)
Transcription/Protein	76 (17)	9 (10)	91 (17)	67 (13)
Transport	24 (5)	3 (5)	28 (5)	37 (7)
Vacuole	0 (0)	0 (0)	2 (0)	12 (2)
Unknown	199 (44)	36 (41)	216 (41)	231 (45)
Total	457	88	523	511

Functional categories are based on the *Candida* Genome Database http://www.candidagenome.org

Table 3

Transcripts upregulated in both intermediate and mature biofilms

Category	Genes (Candida Genome Database)	No. genes in functional category
Amino acid	*AGP2, ARG1, CAN1, CDG1, CPA1, CPA2, SMM1*	6 (5)
Carbohydrate	*CAT8, CIT1, DLD3, FBP1, GAL1, GAL10, HGT1, HGT2, HGT14, KGD1, MLS1, PAM16, PCK1*	13 (10)
Cell wall	*BGL2, CYC3, ECE1, FMP45, orf19.6489*	5 (4)
Cytoskeleton	*SDA1*	1 (1)
DNA/Cell Cycle	*AAH1, orf19.1005, orf19.5845*	3 (2)
Energy/Metabolism	*ALD6, AOX2, ARG8, COX11, COX 17, CTN1, GUT2, ICL1, INO1, NCE103, NDE1, OYE22, OYE23, YAT2, orf19.361*	15 (12)
Fatty Acid	*FAA2, orf19.732*	2 (2)
Heat Shock Protein	*HSP30,*	1 (1)
Hyphal	*RLP1*	1 (1)
Iron	*CFL2, FRE10, ISU1, SIT1*	4 (3)
Plasma Membrane	*ERG25, PDR16*	2 (2)
Resistance/Stress	*AQY1, EBP1, MDR1, SOD6, YHB3*	5 (4)
Transcription/Protein	*CIC1, DBP1, DBP7, MRPL33, MRT4, MSS116, MTO1, PEX4, REX2, RLP7, RPC19 RRN11, SAP5, SOF1, UGA32, orf19.124*	16 (13)
Transport	*GNP1, JEN2, LEU5, OAC1, SFC1, TIM9, TNA1*	7 (6)
Unknown		43 (35)
Total		124

Table 4

Transcripts downregulated in both intermediate and mature biofilms

Category	Genes (Candida Genome Database)	No. genes in functional category
Amino acid	*GLT1*	1 (4)
Carbohydrate	*UGP1, PFK2*	2 (7)
Cell wall	*CWH43, SCW11*	2 (7)
Cytoskeleton	*DYN1, IQG1*	2 (7)
DNA/Cell Cycle	*HHF1, HHF22, HTA2, PCL2, POL30, RNR3, TMP1, orf19.7634*	8 (30)
Plasma Membrane	*ERG7, PLB1*	2 (7)
Unknown		10 (37)
Total		27

Table 5

Comparison of RT-PCR and microarray results for genes of interest

Gene	Microarray Fold Change (Biofilm/Planktonic)	RT-PCR Fold Change (Biofilm/Planktonic)
ALS1	11.8	1370
ARG1	3.3	154.3
BGL2	1.5	3.1
CDR2	1.5	2.6
ECM3	1.8	2.3
ERG25	1.8	21.1
FET3	2.1	19.8
HGT2	52.4	1060
INO1	2.9	13.1
KRE1	1.9	32.7
PCK1	2.2	66.3
PHR1	2.4	24.2
SAP5	2.0	29.5